www.czasopisma.pan.pl PAN POLSKA AKADEMIA NAUK www.journals.pan.pl

Arch. Metall. Mater. **65** (2020), 3, 1081-1086

DOI: 10.24425/amm.2020.133221

TAE-HOON KANG[1], KYU-SIK KIM[1], MIN-JEONG LEE[2],
JUNG-YEUL YUN[2], KEE-AHN LEE[1*]

FABRICATION AND COMPRESSIVE PROPERTIES OF OPEN-CELL Ni-Mo-Cr (HASTELLOY) FOAMS MANUFACTURED BY ELECTROSTATIC POWDER SPRAYING

An open-cell Ni-Mo-Cr foam was newly manufactured using electrostatic powder spraying process and its room-temperature compressive properties were investigated in this study. For manufacturing Ni-Mo-Cr foam, Ni-Mo-Cr powders were sprayed on the polyurethane pre-form by electrostatic powder spraying process. And then, Ni-Mo-Cr powder sprayed pre-forms were sintered at 1200°C, 1250°C, and 1300°C, respectively. The relative densities of Ni-Mo-Cr foams were measured at 4 ~ 5%. Room temperature compressive curves of ESP Ni-Mo-Cr foams represented the typical compressive 3-stages (elastic, plateau, densification) of open-cell metallic foam. As a result of observation of deformed specimen, the fracture mode found to be changed from brittle to ductile as sintering temperature increased. Based on these findings, correlations between structural characteristics, microstructure, and compressive deformation behavior were also discussed.

Keywords: metallic foam, electrostatic powder spraying, Ni-Mo-Cr alloy, sintering, compressive property

1. Introduction

Ni-based superalloy foam has excellent high-temperature mechanical properties, corrosion resistance and high temperature oxidation resistance [1]. Due to such advantages, this alloy foam is used in various structural and functional components such as turbine exhausts, insulation panels, damping components, filters, catalyst supports, and pressure and flow gauge [3]. Cell size and shape are known to be structural factors that determine the mechanical and functional properties of metallic foams. To manufacture metallic foam with Ni-based superalloy, attempts were made using various processes including space holder [4], reduction sintering [5-6] and pack-cementation [7-9] methods. However, these processes have issues of controlling of size and location of cell and inhomogeneous distribution of elemental composition, which lead to the need for a new process.

The replication method is one of the cell designing process of metallic foam. In this method, metal powders are deposited on the metal or polyurethane pre-form by using powder spraying or slurry dipping. And then, sintering process is additionally conducted. Therefore, the replication method can realize free cell design of metallic foam without restrictions [10]. G.J. Davies et al. proposed a powder alloying process that uses this replication method [11]. This powder alloying process sprays metal alloy powder on an electroplated pure metal pre-form surface and applies sintering to manufacture alloy foam. Ni-based superalloy foam fabricated using the powder alloying process can have homogeneous distributions of alloying elements and pore sizes. The authors of this study have investigated the high-temperature mechanical properties and high-temperature oxidation properties of this superalloy foam [12-14]. However, the elemental composition of the superalloy foam fabricated with powder alloying process is controlled by the mass ratio between the pure metal pre-foam and the sprayed alloying powder. As a result, the process has the limitation of requiring accurate control of alloy powder amount during spraying. In addition, as it initially fabricates a pure foam and fabricates the alloy foam separately, the overall cost of the process is also high.

The new electrostatic powder spraying (EPS) process uses corona electrostatic force to adhere negatively charged (–) alloy powders to a positively charged (+) polymer preform, and then applies debinding and sintering processes to fabricate a metallic foam. The alloy powder used for this process has the same composition with metal foam. In addition, the EPS is a dry process that only uses electrostatic forces to directly spray alloying powder on a polymer preform. Compared to conventional

[1] INHA UNIVERSITY, DEPARTMENT OF MATERIAL SCIENCE AND ENGINEERING, INCHEON 22212, REPUBLIC OF KOREA
[2] KOREA INSTITUTE OF MATERIALS SCIENCE (KIMS), CHANGWON 51508, REPUBLIC OF KOREA

* Corresponding author: keeahn@inha.ac.kr

slurry replication (which is one of the typical processes for fabricating metallic foams), the ESP process is not influenced by the viscosity of the slurry. For this reason, structural factors such as relative density, the cell size, or other parameters can be controlled easily through changing the shape and pore size of polyurethane preform. Such advantage of the ESP process allows the fabrication of complex, elaborate metallic foam up to near-net shapes and well-controlled chemical composition of metallic foams. However, studies of the ESP process are currently limited to painting layers and thin film fabrication [15-16], and there is no study investigating the fabrication and mechanical properties of Ni-based superalloy foam using the ESP process.

This study tried to fabricate an open-cell Ni-Mo-Cr (Hastelloy) foam using an electrostatic powder spray process. And the effect of sintering temperatures on the structure and microstructure of Ni-Mo-Cr foam was investigated. The compressive deformation behavior of ESP Ni-Mo-Cr foam was analyzed in correlation to its structural factors. Moreover, the compressive properties of ESP manufactured foams were compared to Ni-based superalloy foams fabricated by other processes.

2. Experimental method

To fabricate the Ni-Mo-Cr (Hastelloy) foam, a polyurethane preform with dimensions of 40 mm length × 40 mm width × 10 mm thickness was used, as depicted in Fig. 1(a). The chemical composition of the powders used in this study was analyzed as Ni-16.46%Mo-15.42%Cr-6.60%Fe-3.06% W-0.03%C (wt.%) by inductively coupled plasma (ICP, 720 Series). The powder had a spherical shape, and the average particle size measured ~34 μm. It was also confirmed that the powder was an alloy powder with all elements evenly distributed (Fig. 1(b)). DC high voltage was applied to the Hastelloy powder and polyurethane preform, charging them with negative (–) charge and positive (+) charge, respectively. And then electrostatic spraying was conducted with the amount of 3.5 kg/m^2 area density. To remove the initial polyurethane from the as-sprayed preform, debinding was performed at 1000°C for an hour in a hydrogen atmosphere. And then, vacuum sintering processes were performed at 1200°C, 1250°C, and 1300°C for an hour, respectively, followed by furnace cooling. Hereafter, each of the Ni-Mo-Cr foams that underwent different sintering temperatures will be referred to as 1200 foam, 1250 foam, and 1300 foam.

In order to identify the structural characteristics of the fabricated Ni-Mo-Cr foams, scanning electron microscopy (SEM, JSM-5500F) was used. The cell size, strut thickness of ESP Hastelloy foams was measured by using an image analyzer (Media Cybernetics Inc., Image-Pro Plus). For the microstructure observation, a standard preparation was conducted including grinding (SiC paper from #400 to #2000) and mirror polishing (alumina slurry up to 1 μm) steps. X-ray diffractometer (XRD, D/MAX RAPID-S) equipment was used for phase analysis of the ESP fabricated foams.

The compression test of ESP Hastelloy foams was conducted at room temperature using INSTRON 8501 equipment. To this end, square-shaped samples, with a length of 10 mm, a width of 10 mm width, and a thickness of 10 mm, were machined using

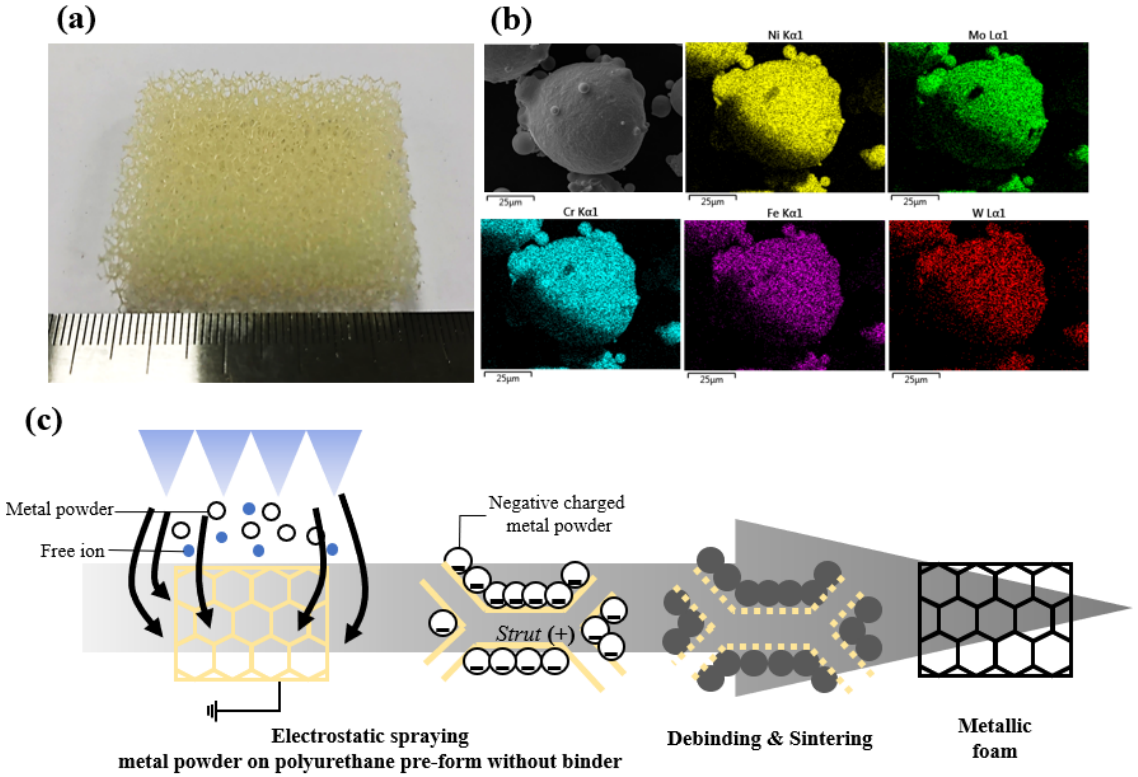

Fig. 1. Macro image of polyurethane pre-form (a) and initial Ni-Mo-Cr alloy powder (b). Schematic diagram of ESP process (c)

wire cutting. The compression tests were performed up to a total strain (ε_t) of 0.6 with a strain rate of 1×10^{-3} /s. Three samples for each sintering condition were used to confirm representative properties. After the compression test, the deformed specimens were observed using SEM.

3. Results and discussion

Fig. 2((a), (c), (e)) shows the representative strut structure of ESP Ni-Mo-Cr foams observed by using SEM. The unit cell featured a tetrakaidecahedron structure composed of pentagons and hexagons. Such a structure is formed due to the shape of the polyurethane preform. Meanwhile, some edge defects (white arrows) were observed on the surfaces of Ni-Cr-Mo foams. The formation of edge defects is known to be caused by the difference of heat expansion coefficients between metal powders and the polyurethane preform during sintering [17]. Those defects were mainly observed in 1200 foam and 1250 foam but were not found in 1300 foam which sintered at the highest sintering temperature. Average cell sizes of Ni-Mo-Cr foams were measured as 2322 μm (sintered at 1200°C), 2410 μm (1250°C), and 2522 μm (1300°C), respectively. It is noteworthy that the average cell size increased as sintering temperature increased. On the other hand, the average strut thickness was measured as 360 μm (1200 foam), 343 μm (1250 foam), and 335 μm (1300 foam). The thickness of strut in the foam decreases as sintering temperature increased.

The relative density of the porous metal can be calculated using the following formula [5-6]:

$$relative\ density = \rho^*/\rho_s \times 100 \quad (1)$$

ρ_s means the density of bulk material, and ρ^* means the density of porous metal. The relative densities calculated using this formula were 1200 foam: 4.11% 1250 foam: 4.17% and 1300 foam: 4.97%. The strut density increased with increasing sintering temperature (as shown in Fig. 2 and Fig. 3). Moreover, the overall volume of porous metal (apparent volume) significantly decreased at 1300°C because of sintering shrinkage. The weights of foams were similarly maintained regardless of sintering temperature. For this reason, the relative density of 1300 foam had a relatively higher value compared to those of 1200 and 1250 foams. Also, cell shape is a factor that can anticipate anisotropy in the mechanical properties of a porous metal. Cell shape can be quantified using cell shape factor (F), and this can be represented as follows [17]:

$$F = \frac{4\pi A}{\theta^2} \quad (2)$$

A is the area of the cell, and Θ is the perimeter of the cell, which has a range of 0-1. The cell shape factors of the Ni-Mo-Cr foams fabricated for this study measured the same at 0.91. Also, this means that it is possible to expect isotropic mechanical properties. Table 1 lists the structural factors of the foams presented above.

TABLE 1

Structural factors of ESP Ni-Mo-Cr foams manufactured in this study

Sample	Sintering temperature (°C)	Relative density (%)	Cell size (μm)	Strut thickness (μm)
1200 foam	1200	4.11	2322	360
1250 foam	1250	4.17	2410	343
1300 foam	1300	4.97	2522	335

Fig. 2((b), (d), (f)) shows surface morphologies of 1200 foam, 1250 foam and 1300 foam. In the case of 1200 foam, the electrostatic sprayed Ni-Mo-Cr powder maintained a spherical shape

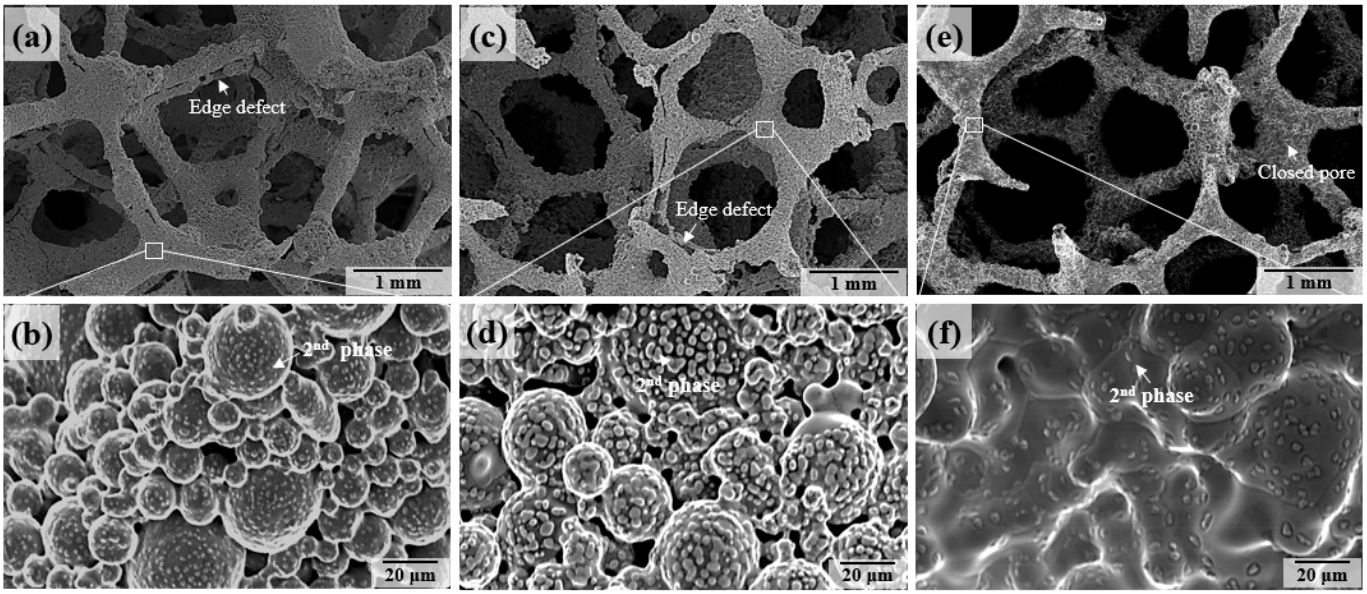

Fig. 2. SEM showing cell morphology and strut surface of Ni-Mo-Cr foams: different sintering temperatures of 1200°C (a-b), 1250°C (c-d) and 1300°C (e-f)

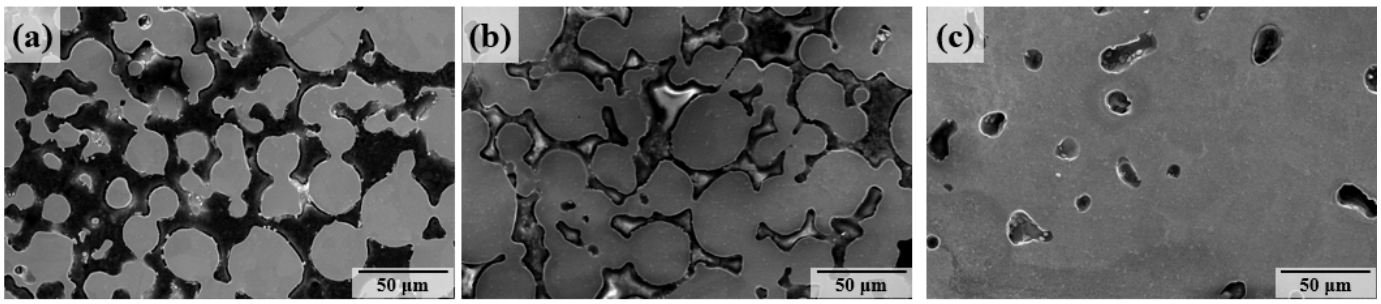

Fig. 3. SEM showing cross-section of Ni-Mo-Cr foams: different sintering temperatures of 1200°C (a), 1250°C (b) and 1300°C (c)

(initial powder shape) even after sintering (Fig. 2(b)), and narrow sintering neck was formed between powders. The surface morphology of 1250 foam (Fig. 2(d)) was similar to 1200 foam showing initial powder shape and narrow sintering necks. Meanwhile, 1300 foam, which sintered at highest sintering temperature, had a smoother strut surface compared to 1200 foam and 1250 foam.

Fig. 3 shows cross-sectional SEM microstructures according to the sintering temperature. As sintering temperature increased, denser microstructures were observed. In general, powder sintered bulk Ni-Mo-Cr alloy is known to perform up to 4 hours of sintering at 1000°C-1200°C for densification [19]. However, if the same sintering condition is applied to a metallic foam, cells can collapse due to low structural stability of struts. As confirmed in this study, a shorter sintering time at a higher sintering temperature is suitable for fabricating dense foam. Meanwhile, a second phase with a size of ~3 µm was observed on the strut surface of ESP Ni-Mo-Cr foam. This second phase had a block shape that was found in locations regardless of grain and grain boundary. Fig. 4 shows the results of the phase analysis. The second phase was identified as (Cr, Mo)-rich carbides by a combination of EDS point analysis (Fig. 4(a)) and XRD pattern analysis (Fig. 4(b)).

Fig. 5(a) is the compressive stress-strain curves of ESP Ni-Mo-Cr foams. The compressive mechanical responses of ESP foams show typical stress-strain behaviors of the metallic foam which include three different stages: linear elastic stage, plateau (pore collapse) stage and densification stage [5-6]. Compressive yield strengths ($\sigma^*_{y.s.}$) measured as 0.09 MPa (1200 foam), 0.16 MPa (1250 foam), and 0.42 MPa (1300 foam), respectively. The compressive strength of Hastelloy foams increased as sintering temperature increased. Relative stress of ESP foams was represented as a function of relative density and compared with other Ni-based superalloy foams in Fig. 5(b). Here, the relative stress was calculated by using the equation of $\sigma^*_{y.s.}$ (yield strength of foam)/$\sigma_{y.s.}$ (yield strength of bulk material), and this value is suited for comparing physical properties between foams. The relative compressive strengths of ESP foams fabricated in this study were relatively lower than foams reported by other studies. However, it is noteworthy that the values became similar to sintering temperature increased (1300 foam). This result confirms that the possibility of being able to properly fabricate Ni-Mo-Cr foam with electrostatic powder spraying using only sintering temperature conditions.

Fig. 6 shows representative deformed and fractured structures of ESP foams with different sintering temperatures. In the case of 1200 and 1250 foams (sintered at lower sintering temperature), cracks were observed along the sintering neck (white arrow). The pre-existing edge defects in 1200 and 1250 foams could cause premature fractures and cracking strut in the early stage of the compression test. On the other hand, in 1300 foam (sintered at highest sintering temperature), fine dimples of ductile

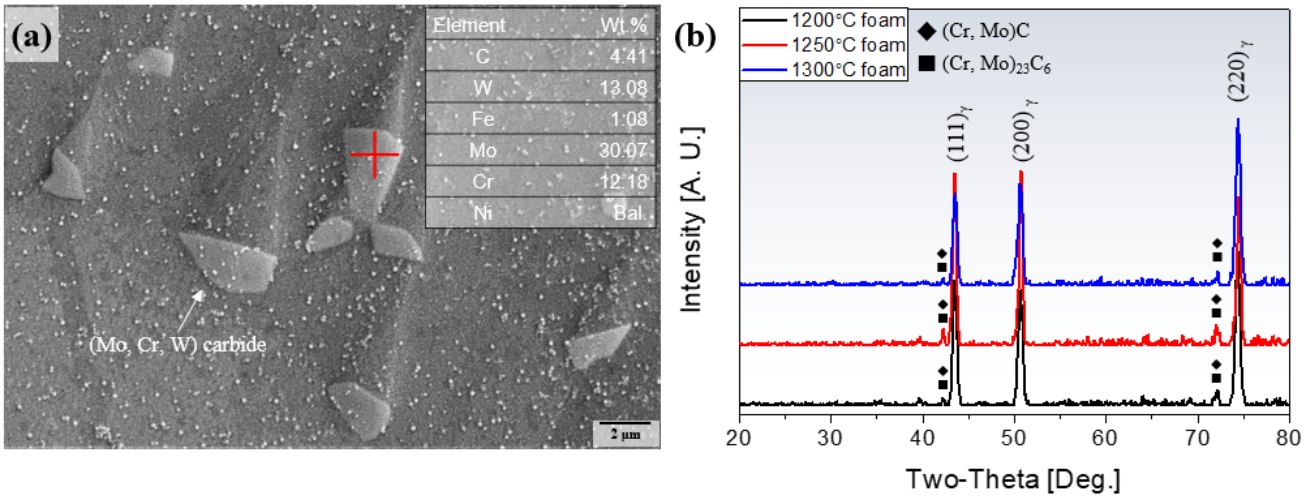

Fig. 4. SEM showing morphology of carbide of 1300 foam (a) and XRD result of Ni-Mo-Cr foams (b)

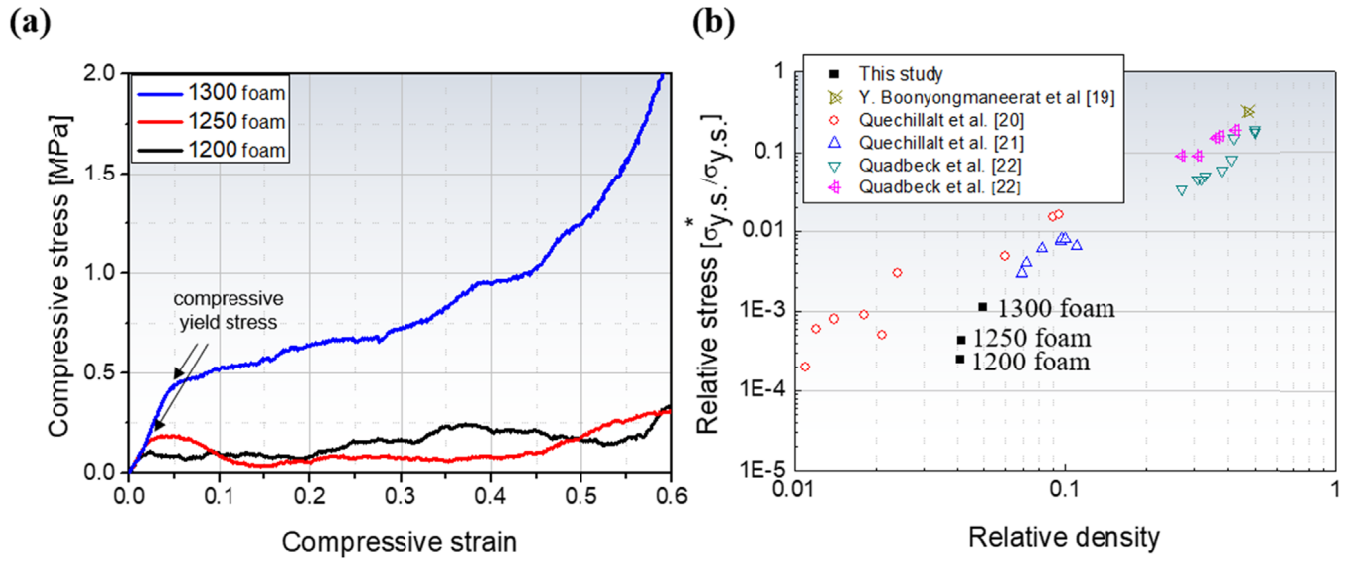

Fig. 5. Compressive stress-strain curves of ESP Ni-Mo-Cr foam (a) and comparison of relative density of Ni-based superalloy foams fabricated with various manufacturing processes (b)

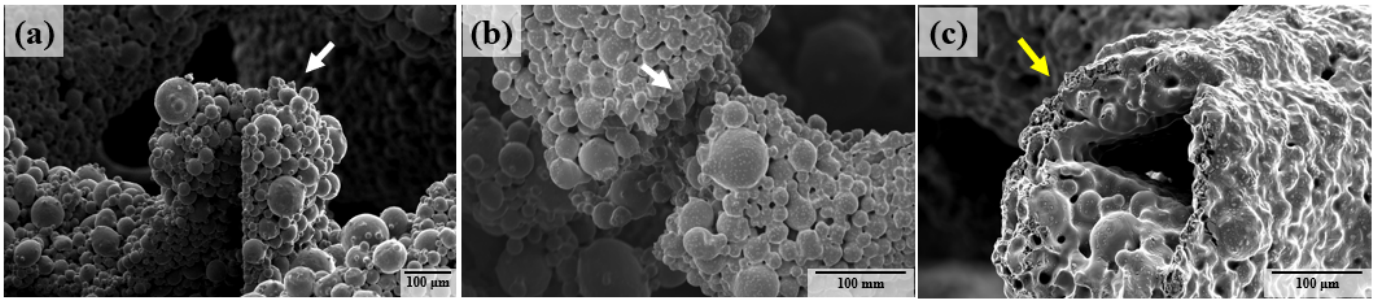

Fig. 6. SEM image of compressed foams: 1200 foam (a), 1250 foam (b) and 1300 foam (c)

fractures were observed (yellow arrow). This feature confirms that the brittle fracture turns into ductile fracture as sintering temperature increased. Based on these findings, this study was able to fabricate a sound Ni-Mo-Cr foam using electrostatic powder spraying and sintering processes.

4. Conclusions

This study tried to fabricate an open-cell Ni-Mo-Cr (Hastelloy) foam using an electrostatic powder spray process. And the effect of sintering temperatures on the structure and microstructure of Ni-Mo-Cr foam was investigated. In summary, the following key conclusions were obtained. Ni-Mo-Cr foam was fabricated using powder with an average particle size of 34 μm. The unit cell consisted of tetrakaidecahedron, and the cell size increased to 2322 μm, 2410 μm and 2522 μm, but strut thickness decreased to 360 μm, 343 μm and 335 μm as the sintering temperature increased. The interior of the microstructure was confirmed to have formed a (Mo, Cr) carbide-reinforced phase. A room-temperature compression test confirmed that compressive stress-strain curves with three stages (linear elastic stage, pore collapse stage, densification stage) were characterized. The compressive strength increased significantly as sintering temperature increased. After implementing compressive deformation, observation of the specimen identified brittle fractured surfaces along the sintering neck in the 1200 foam, and the fracture changed to a ductile fractured surface as sintering temperature increased.

Acknowledgements

This work was supported by INHA UNIVERSITY Research Grant.

REFERENCES

[1] J.R. Davis, Nickel, Cobalt, and Their Alloys, ASM specialty Handbook, ASM International (2000).

[2] W.F. Smith, Structure and properties of engineering alloys, 2nd ed., McGraw-Hill (1981).

[3] H. Choe, D.C. Dunand, Acta Mater. **52**, 1283 (2004).

[4] I. Unver, H.O. Gulsoy, B. Aydemir, JMEPEG **22**, 3755 (2013).

[5] L.J. Gibson, M.F. Ashby (2nd Ed.), Cellular solids: Structure and Properties, Cambridge University Press, Cambridge (1997).

[6] M.F. Ashby, A.G. Evans, N.A. Fleck, L.J. Gibson, J.W. Hutchinson, H.N.G. Wadley, Metal Foams: A Design Guide, Elsevier, Oxford (2000).
[7] T.J. Lu, H.A. Stone, M.F. Ashby, Acta Mater. **46**, 3619 (1998).
[8] T.J. Lu, Int. J. Heat Mass Transfer. **42**, 2031 (1999).
[9] J. Banhart, Pro. Mater. Sci. **46**, 559 (2001).
[10] M.A. Atwater, L.N. Guevara, K.A. Darling, M.A. Tschopp, Adv. Eng. Mater. **20**, 1700766 (2018).
[11] G.J. Davies, S. Zhen, J. Mater. Sci. **18**, 1899 (1983).
[12] J.S. Oh, Y.M. Kong, B.K. Kim, K.A. Lee, J. Kor. Powd. Met. Inst. **21**, 55 (2014).
[13] J.S. Oh, M.C. Shim, M.H. Park, K.A. Lee, Met. Mater. Int. **20**, 915 (2014).
[14] K.S. Kim, J.Y. Yun, B.G. Choi, K.A. Lee, Met. Mater. Int. **20**, 507 (2014).
[15] Q. Ye, J. Domnick, Powder Technol. **135-136**, 250 (2003).
[16] W. Bao, Q. Chang, R. Yan, G. Meng, J. Membrane Sci. **252**, 175 (2005).
[17] A.W. Orłowicz, M. Mróz, M. Tupa, A. Trytek, Arch. Foundry Eng. **15**, 75 (2015).
[18] P.C. Angelo, Powder Metallurgy: Science, Technology and Applications, Prentice-Hall of India, New Delhi (2008).
[19] Y. Boonyongmaneerat, D.C. Dunand, Adv. Eng. Mater. **10**, 379 (2008).
[20] D.T. Queheillalt, D.D. Hass, D.J. Sypeck, H.N.G. Wadley, J. Mater. Res. **16**, 1028 (2001).
[21] D.T. Queheillalt, Y. Katsumura, H.N.G. Wadley, Scr. Mater. **50**, 313 (2004).
[22] P. Quadbeck, J. Kaschta, R.F. Singer, Adv. Eng. Mater. **6**, 635 (2004).